Orientation masking and cross-orientation suppression (XOS): Implications for estimates of filter bandwidth

Tim S. Meese
School of Life and Health Sciences, Aston University, Birmingham, UK

David J. Holmes
School of Life and Health Sciences, Aston University, Birmingham, UK

Most contemporary models of spatial vision include a cross-oriented route to suppression (masking from a broadly tuned inhibitory pool), which is most potent at low spatial and high temporal frequencies (T. S. Meese & D. J. Holmes, 2007). The influence of this pathway can elevate orientation-masking functions without exciting the target mechanism, and because early psychophysical estimates of filter bandwidth did not accommodate this, it is likely that they have been overestimated for this corner of stimulus space. Here we show that a transient 40% contrast mask causes substantial binocular threshold elevation for a transient vertical target, and this declines from a mask orientation of 0° to about 40° (indicating tuning), and then more gently to 90°, where it remains at a factor of ~4. We also confirm that cross-orientation masking is diminished or abolished at high spatial frequencies and for sustained temporal modulation. We fitted a simple model of pedestal masking and cross-orientation suppression (XOS) to our data and those of G. C. Phillips and H. R. Wilson (1984) and found the dependency of orientation bandwidth on spatial frequency to be much less than previously supposed. An extension of our linear spatial pooling model of contrast gain control and dilution masking (T. S. Meese & R. J. Summers, 2007) is also shown to be consistent with our results using filter bandwidths of ±20°. Both models include tightly and broadly tuned components of divisive suppression. More generally, because XOS and/or dilution masking can affect the shape of orientation-masking curves, we caution that variations in bandwidth estimates might reflect variations in processes that have nothing to do with filter bandwidth.

Keywords: human vision, psychophysics, contrast gain control, orientation bandwidth, XOM, spatial summation

Citation: Meese, T. S., & Holmes, D. J. (2010). Orientation masking and cross-orientation suppression (XOS): Implications for estimates of filter bandwidth. *Journal of Vision, 10*(12):9, 1–20, http://www.journalofvision.org/content/10/12/9, doi:10.1167/10.12.9.

Introduction

One of the most striking features of mammalian visual cortex is its selectivity for the orientation of luminance contours. This property was first revealed in laboratory animals by the pioneering single-cell physiology of Hubel and Wiesel (1959) but has since found much support psychophysically in humans (Blakemore & Campbell, 1969; Blakemore & Nachmias, 1971; Campbell & Kulikowski, 1966; Georgeson & Shackleton, 1994; Greenlee & Heitger, 1988; Houlihan & Sekuler, 1968; Määttänen & Koenderink, 1991; Movshon & Blakemore, 1973; Pantle & Sekuler, 1969; Phillips & Wilson, 1984; Snowden, 1992; Thomas & Gille, 1979).

One particularly influential psychophysical paradigm has been that of orientation masking where a target stimulus—often a patch of sine-wave grating—is detected in the presence of a mask stimulus, often another patch of sine-wave grating. When the target and mask have similar spatial characteristics, the mask is said to be a pedestal and threshold elevation occurs at moderate contrasts and above (Legge & Foley, 1980; Nachmias & Sansbury, 1974; Wilson, 1980). However, when the mask and target have orthogonal orientations, the effect is abolished, at least at high spatial frequencies (Campbell & Kulikowski, 1966; Daugman, 1984; Harvey & Doan, 1990). This masking technique is also a widely cited method for measuring the orientation bandwidths of spatial filters. The approach measures the variation of masking with the relation between mask and target orientations to gauge the selectivity of the underlying contrast detecting mechanisms (Phillips & Wilson, 1984). However, how secure are previous conclusions about bandwidth using this method? To tackle this, we must first consider some details of masking models.

Within-channel masking: The sigmoidal contrast transducer and multiplicative noise

The standard model of masking from the 1980s supposes an initial linear filtering stage followed by a nonlinear transducer (a point-wise nonlinearity) and additive noise (Legge & Foley, 1980; Wilson, 1980). The transducer is sigmoidal, accelerating at low contrasts but compressing

doi: 10.1167/10.12.9 Received June 19, 2009; published October 8, 2010 ISSN 1534-7362

for moderate input levels and above. Thus, a mask that keeps the drive within the accelerating part of the transducer causes facilitation, whereas one that pushes the transducer into compression will cause masking, consistent with abundant psychophysical data (e.g., Legge & Foley, 1980; Wilson, 1980). An alternative model of masking—one that in many circumstances is equivalent to the nonlinear transducer model—allows for a linear (or other) transducer but invokes multiplicative noise (Burton, 1981; Tolhurst, Movshon, & Dean, 1983). In this model, as the input to the target mechanism increases then so does the variance of the noise, which makes the target more difficult to detect. Thus, both models propose that masking occurs when the detecting mechanisms are substantially stimulated by the mask, and that this reduces the signal-to-noise ratio for the target. The type of masking described above is sometimes called *within-channel* masking. In what follows, we discuss this in terms of response compression, but the arguments apply equally to the multiplicative noise model.

Phillips and Wilson (1984) used the within-channel model to estimate the orientation bandwidths of the underlying detecting mechanisms (spatial filters). One notable feature of their work is that the compressive region of contrast transduction means that psychophysical masking functions can have broader bandwidths than those of the underlying mechanisms. Nevertheless, Phillips and Wilson's (1984) estimates of mechanism bandwidth (half-width at half-height) were fairly broad at low spatial frequencies (0.5 c/deg), being a little over ±30°. At higher spatial frequencies, they decreased to a little under ±20°. This has led to a long-standing belief that orientation bandwidths decrease with spatial frequency. A view fueled by reports from single neuron studies that *spatial frequency* bandwidths tend to decrease with preferred spatial frequency (Baker, Thompson, Krug, Smyth, & Tolhurst, 1998; DeValois, Albrecht, & Thorell, 1982; Tolhurst & Thompson, 1981; Yu et al., 2010).

Cross-channel and pre-channel masking

In spite of the early success of the static nonlinear transducer model, there is good psychophysical evidence that at least some aspects of masking do not arise from within-channel excitation from the mask. For example, Foley (1994) measured contrast discrimination thresholds in the presence of a fixed contrast mask whose orientation was different from that of the target. The presence of the fixed mask transformed the conventional dipper function: at low pedestal contrasts, increment thresholds were increased (the fixed mask produced masking), but the upper limb of the dipper function was relatively untouched by the fixed mask. Crucially, however, the region of facilitation remained a distinct feature of the transformed dipper function. Analogous results have been found by Holmes and Meese (2004), Mullen and Losada (1994), and Ross, Speed, and Morgan (1993). These results do not fit with the idea of within-channel masking and a static sigmoidal transducer because in that case, a consequence of the fixed mask would be to drive the input beyond the accelerating region of the output transducer, and facilitation should not occur.

Further evidence against the within-channel model of masking comes from experiments in which masking functions have been measured for mask components of different orientations. In this case, the model predicts lateral translations (on a log axis) of dipper functions. However, as orientation difference increases, the magnitude of facilitation also decreases (Foley, 1994; Ross & Speed, 1991; Zenger & Sagi, 1996), which is inconsistent with the model. Importantly, and contrary to some of the masking studies above, several studies have found that threshold elevation occurs even for orthogonally oriented masks (e.g., Burbeck & Kelly, 1981; Ferrera & Wilson, 1985; Foley & Chen, 1997; Foley, 1994; Meese, 2004; Ross & Speed, 1991). If detecting mechanisms are orientation tuned as previously supposed, then this result cannot be explained in terms of within-channel masking. Meese and Holmes (2007) measured cross-orientation masking (XOM) for a wide range of spatial and temporal frequencies and found that it was greatest at low spatial and high temporal frequencies (Burbeck & Kelly, 1981; Medina & Mullen, 2009; Meese & Baker, 2009; Meese & Hess, 2004; Meese & Holmes, 2007; Meese, Summers, Holmes, & Wallis, 2007). This reconciled different conclusions regarding XOM across a large body of psychophysical studies (see Meese & Holmes, 2007 for meta-analysis).

Another argument against the within-channel interpretation of masking involves the slope of the psychometric function. At contrast detection threshold (without a mask), this is fairly steep, consistent with an accelerating contrast transducer (Lu & Dosher, 2008; Meese & Summers, 2009). This slope is barely affected, if at all, by cross-oriented masks (Meese & Baker, 2009; Meese, Challinor, & Summers, 2008; Meese & Holmes, 2007). If the mask were to drive the target up the transducer, then the psychometric slope should become shallow (a d' slope of unity) owing to the approximately linearizing effect this has for small signal increments (Foley & Legge, 1981; Meese, Georgeson, & Baker, 2006). Overall then, an explanation of XOM in terms of within-channel masking within isotropic (or similar) detecting mechanisms seems unlikely.

An alternative model (here called the *suppression model,* but sometimes, the *contrast gain control model*) can accommodate the failings of the within-channel model and was suggested by Foley (1994). In this model, the response of the detecting mechanism (*resp*) is an accelerating function of its input (C_t^p, with exponent p typically ≥ 2). This is divided by the sum of a string of weighted terms: a constant (z), a copy of the excitatory term raised to an exponent (q), and a contribution from $i = 1$ to λ mask

components (with contrast M) outside the excitatory passband, also raised to the exponent q, where $(p - 1) < q < p$. Thus, a typical functional form of the suppression model is

$$resp = C_t^p/(z + C_t^q + \sum_{i=1:\lambda} w_i M_i^q), \quad (1)$$

though implementations vary in detail.

Crucially, the M-type terms allow the model to accommodate the empirical results reviewed above. For example, a mask can cause masking without facilitation through this pathway, and it can elevate the region of facilitation produced by a pedestal (Foley, 1994). This pathway also leaves the shape of the psychometric function (largely) intact. This is because suppression from this pathway is equivalent merely to increasing the size of the saturation constant z, meaning the contrast response at detection threshold remains an accelerating one (determined by p) and the psychometric function remains steep.

When the drive from the M-type terms is conceived as arising from the outputs of other spatially tuned channels (Albrecht & Geisler, 1991; Heeger, 1992), this arrangement is sometimes referred to as a *cross-channel* masking model. Broadly speaking, this model is also consistent with single-cell work in the primary visual cortex, which finds cross-orientation inhibition between orthogonal gratings and bars (Bonds, 1989; Carandini, Heeger, & Movshon, 1997; Morrone, Burr, & Maffei, 1982; Ramoa, Shadlen, Skottun, & Freeman, 1986; Tolhurst & Heeger, 1997).

A potential misconception

Note that in the suppression model (Equation 1), there are two main components to suppression: self-suppression and that from the nonexcitatory pool (the M-type terms), sometimes called cross-orientation suppression (XOS). Without the M-type terms, this model is identical to typical implementations of the within-channel model of masking by the static nonlinear transducer (Legge & Foley, 1980). Nevertheless, it is inappropriate to think of this model as the sigmoidal transducer *plus* a contribution from broadly tuned suppression. That would involve an equation for sigmoidal transduction divided by a broadly tuned suppressive term. Instead, Equation 1 places the broadly tuned suppression on the denominator of the equation along with self-suppression. Thus, it actually describes a purely accelerating contrast transducer that is susceptible to a variety of suppressive interactions.

However, there are model formulations for which a static sigmoidal output transducer might survive. One example is a model in which cross-orientation suppression is placed *before* the orientation tuning of the detecting mechanism. We refer to this as a *pre-channel* model of masking. One such model involves a general suppressive field in the retina (Shapley & Victor, 1978; Solomon, Lee, & Sun, 2006) or LGN (Alitto & Usrey, 2008; Bonin, Mante, & Carandini, 2005; Nolt, Kumbhani, & Palmer, 2007; Webb, Dhruv, Solomon, Tailby, & Lennie, 2005), which can also accommodate interactions that lie outside the passband or footprint of the subcortical classical receptive field (Meese & Hess, 2004). This might be characterized by an equation with a form similar to Equation 1 but implemented before orientation (cortical) filtering.

Orientation tuning revisited

The empirical and theoretical work reviewed above raises some issues for previous masking studies that have assumed a within-channel model of masking (e.g., Phillips & Wilson, 1984). First, what effect does the process of XOS have on estimates of orientation bandwidths in such studies? Second, since the phenomenon of cross-orientation masking (XOM) is greatest for masks and targets with low spatial frequency and high temporal frequency, might there be a systematic effect of these parameters on previous estimates of bandwidth?

To address these issues here, we report an orientation-masking study using a forced-choice procedure over a wide range of finely sampled (10°) orientation differences (0°–90°), a wide range of spatial frequencies (1–9 c/deg), and two different temporal conditions (sustained and transient). We are aware of no earlier study of orientation masking that has considered such a wide range of conditions (see General discussion section for further details), though a study performed while this one was in preparation is closely related (Cass, Stuit, Bex, & Alais, 2009) and we shall return to it in the General discussion section.

Arguably, we might have limited our reanalysis to the results of Phillips and Wilson (1984) using Foley's (1994) estimate of broadly tuned suppression in the model. However, in contrast to Phillips and Wilson's study, there was no tightly tuned component of orientation masking in Foley's data (see forward to Figure 9), making this an unpromising starting point. Furthermore, Foley measured only coarsely sampled orientation-masking functions (for a range of mask contrasts) at only a single spatiotemporal frequency. We comment on this further in the discussion.

Preview

Our motivation was to revisit orientation tuning in human vision using a masking paradigm. We wanted to know whether extending a Phillips and Wilson (1984) type model to include a purely suppressive route to masking would change our interpretation of orientation masking. Our results here confirm that XOM is found primarily for transient stimuli and only at low or middle spatial frequencies. Our transient data and those of Phillips and Wilson are well fitted by the model described above, which incorporates two components of suppression: one very broadly tuned, the other quite narrowly tuned.

Assuming that the narrowly tuned component is coupled to excitatory selectivity, we conclude that filter bandwidths (for the data from both studies) are narrower than those estimated by Phillips and Wilson at low spatial frequencies, and fairly constant with spatial frequency (~±20°), though some uncertainty remains at the higher spatial frequencies. More generally though, we present arguments for caution when interpreting bandwidths from masking data.

Methods

Observers

The two authors served as observers (TSM and DJH). Both were well practiced with the stimuli before data collection began and had normal or optically corrected-to-normal vision.

Equipment

Stimuli were displayed using a VSG2/3 (Cambridge Research Systems, UK) graphics board operating in pseudo 12-bit mode under the control of a Pentium PC. The monitor was a Sony Trinitron Multiscan 200PS driven at 120 Hz and had a mean luminance of 70 cd/m^2.

Observers were seated in a darkened room, with their head in a chin and headrest, and viewed the stimuli binocularly from a distance of either 114 cm or 228 cm.

Stimuli

Mask and target stimuli were sine-wave gratings that were spatially modulated by raised cosine and Gaussian functions, respectively (Figure 1). They were in sine phase with a small central dark fixation point (2 × 2 pixels square) that was visible throughout the experiment. Masks had a full-width at half-height of 4.4 deg with a central plateau of 3.8 deg, and targets had a full-width at half-height of 1.67 cycles. The targets were always oriented vertically. There were two temporal conditions. In a transient condition, the stimuli were modulated by a single cycle of a 15-Hz square wave (i.e., a positive pulse followed by a negative pulse—see Meese & Baker, 2009 or Meese & Holmes, 2007). In a sustained condition, the stimuli were linearly ramped on and off, had a total duration of 1000 ms, and had a central plateau of 500 ms. The mask and target always had the same temporal modulation and the same spatial frequency, which was 1 c/deg, 3 c/deg, or 9 c/deg.

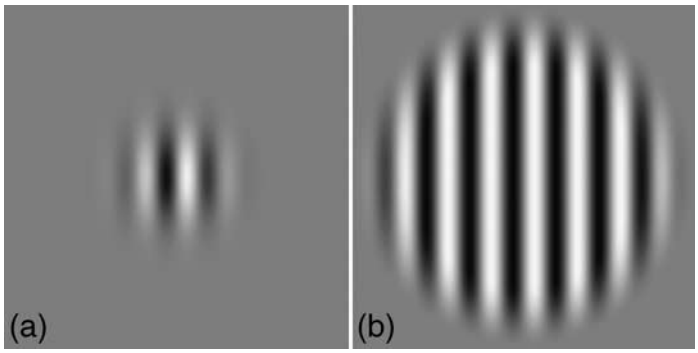

Figure 1. (a) Target Gabor stimulus. (b) Sample grating mask stimulus. Other masks had different orientations. The size of the target was scaled with spatial frequency. The diameter of the mask was the same at all spatial frequencies. The relative sizes shown here are for the 1 c/deg condition.

Stimulus contrast was controlled using lookup tables, and gamma correction ensured linearity over the full contrast range. Mask and target contrasts were controlled independently using a frame-interleaving technique. This put an upper contrast limit of 50% on each of the mask and target components. Mask and target contrasts are expressed in percent and in decibels (dB), defined as $20\log_{10}(C\%)$, where $C\%$ is Michelson contrast in percent, given by $100(L_{max} - L_{min})/(L_{max} + L_{min})$, where L is luminance. The mask contrast was either 0% (baseline) or 40%. Threshold elevation was calculated by subtracting the baseline threshold from the masked threshold, expressed in dB.

Procedure

A temporal two-interval forced-choice (2IFC) paradigm was used, where the mask was presented in both intervals, but the target was presented in only one, selected at random. Observers used mouse buttons to indicate which interval contained the target and were given auditory feedback on their accuracy on each trial. The duration between the offset of the first interval and the onset of the second interval was 500 ms.

Spatial and temporal frequencies were varied across sessions. Mask orientation was interleaved within session and across sessions. In one session, masks were oriented at 0°, 20°, 40°, 60°, and 80°, and in the other, they were oriented at 10°, 30°, 50°, 70°, and 90°. The orientation conditions were split across sessions to produce reasonable session durations, which were about 30 or 40 min for the sustained stimuli. For DJH, the different masks within a session were interleaved across trials. For TSM, they were blocked. Unmasked thresholds were also measured in each session. A full data set was gathered for DJH, and this was used to guide a revised sampling regime for TSM.

Within each experimental session, a pair of interleaved staircases (using a 3-down, 1-up configuration) tracked performance for each mask condition. Each staircase began

with a large step size of 12 dB. This was reduced to 3 dB after the first reversal, where it remained for the remainder of the session. Each staircase terminated after 12 reversals of direction (~48 trials). The data were pooled across the staircase pair (~96 trials) before using probit analysis (Finney, 1971) to estimate a threshold (75% correct). In the rare instances where the standard error of the probit fit was greater than 3 dB, the data were rejected and the condition repeated. The entire experiment was repeated five times and results are plotted as the mean and standard error (±1 *SE*) of the five threshold estimates.

Results, model, and discussion

Orientation-masking functions are shown in Figure 2 for TSM and DJH and are replotted for SL and WS from Phillips and Wilson (1984) in Figure 3. Note the broader range of mask orientations used in the present study. Note also the slightly different spatial frequencies (Figures 2 and 3, rows) and different temporal frequencies (Figures 2 and 3) used in the two studies. In both studies, the transient conditions (solid circles) produced considerably more masking than did the sustained condition (open circles) for spatial frequencies of 3 c/deg and below. At higher spatial frequencies (8 and 9 c/deg), results from the two temporal conditions were similar, though masking was weak in the study here (Figures 2e and 2f).

The data from Phillips and Wilson's (1984) study (Figure 3) do not extend beyond a mask orientation of 45° and so do not indicate whether cross-orientation suppression was involved. However, the data from our own study are clear on this point. In the sustained condition, XOM was weak or absent at all spatial frequencies, but in the transient condition, it was substantial at 1 and 3 c/deg, raising thresholds by up to a factor of 4 (for a mask orientation of 90°). In these conditions, as the difference between mask and target orientations increased, then threshold elevation first decreased fairly steeply and then beyond a mask orientation of 30° or 45°, much more gently, suggesting that two distinct masking processes might be involved. Note that tuning is evident in the data sets from both studies. However, although clear at 8 c/deg in Phillips and Wilson's study (Figures 3e and 3f), there was very little evidence for this at 9 c/deg in the present study (Figures 2e and 2f). The reasons for this difference are not clear, but there are several methodological differences between the studies that might be important (see Figures 2 and 3 for details). The use of a central fixation point here might also be relevant; it is possible that this contributed to masking in the baseline condition at the high spatial frequency, thereby reducing our assessment of the experimental effect (Summers & Meese, 2009).

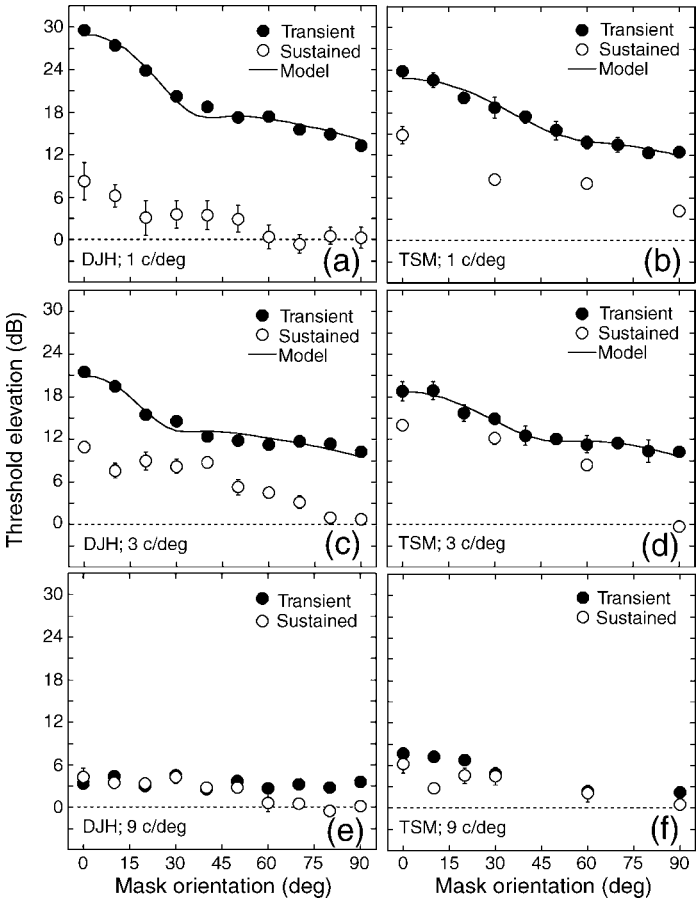

Figure 2. Orientation-masking functions for three different spatial frequencies (rows), two different temporal envelopes (symbols), and two different observers (columns). The transient modulation was a single cycle of a 15-Hz square-wave pulse. The sustained modulation was a 250-ms linear ramp on, followed by a 500-ms plateau, followed by a 250-ms linear ramp off. Targets were vertical sine-phase Gabor patches (1.67 cycles at half-height) and masks were sine-wave gratings. Viewing was binocular and mean luminance was 69.8 cd/m^2. The solid curves are model fits to the 1 and 3 c/deg transient conditions described in the text. Error bars show ±1 *SE* when larger than symbol size (n = 5). Contrast detection thresholds for DJH and TSM, for 1 to 9 c/deg, respectively, were 1.5, 8.5, 25.9 dB and 0, 5.7, 22.3 dB for the transient condition. For the sustained condition, they were 3.6, 4.7, 15.3 dB and −1.1, 0.8, 15.5 dB.

Note that the temporal frequency and spatial frequency effects of XOM reported by Meese and Holmes (2007) are both replicated here: XOM is greatest at high temporal frequencies (transient condition) and low spatial frequencies. Note also that there is no indication of a notch in any of the masking functions in our study around a mask orientation of 45° (Figure 2) as might have been anticipated from the VEP study of Regan and Regan (1987). In that study, it was concluded that cross-orientation

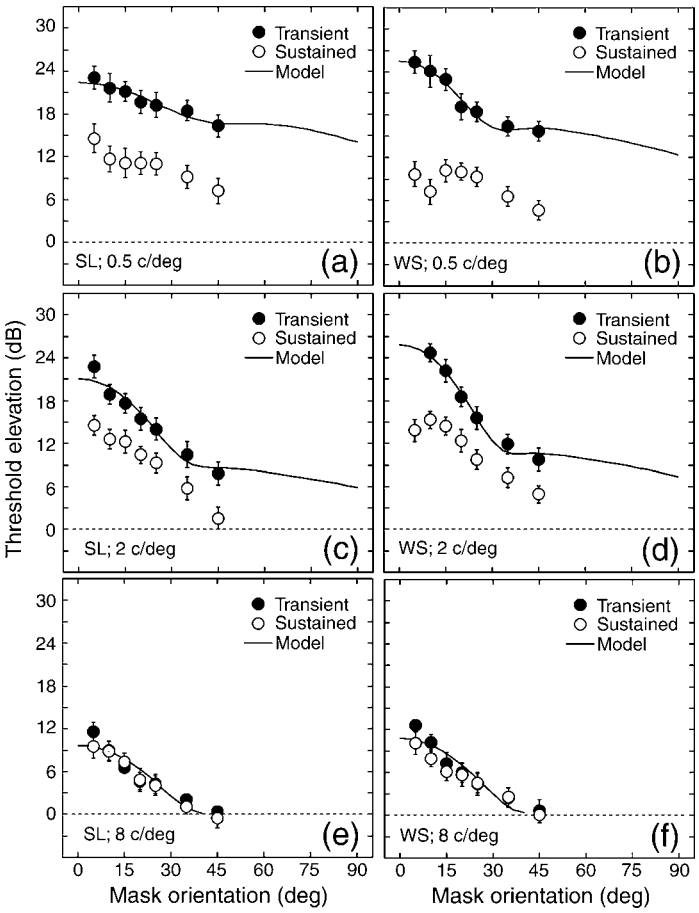

Figure 3. Orientation-masking functions for three different spatial frequencies (rows), two different temporal envelopes (symbols), and two different observers (columns). Data are replotted from Phillips and Wilson (1984). The transient modulation was a single cycle of an 8-Hz square-wave pulse for the target and a 1-s ramped 8-Hz sine wave for the mask. The sustained modulation was a 1-s Gaussian modulation for the target and a single cycle of a 1-Hz sine wave for the mask. Targets were vertical sixth derivatives of a Gaussian and masks were cosine gratings. Viewing was monocular and mean luminance was 17.2 cd/m^2. The solid curves are model fits to the transient conditions described in the text. Error bars show ±1 *SE* when larger than symbol size.

interactions are limited to the orthogonal case. Like single-cell physiology (Bonds, 1989), psychophysical XOM is clearly not restricted in the same way.

Model

Our functional model has similar origins to that used by Phillips and Wilson (1984) but is extended to include a purely suppressive pathway (e.g., Foley, 1994). In other words, it is developed from Equation 1 to handle the broad range of mask orientations used here.

The contrast response of a target mechanism (*resp*) is given by

$$resp = E/(1 + I), \tag{2}$$

where E and I are functions of mask and test contrast and the difference in mask and test orientation as described below.

We assume a Gaussian function (G) for the orientation tuning of the excitatory mechanism. Specifically

$$G = \exp\left(\frac{-diff^2}{2(|h|/1.18)^2}\right), \tag{3}$$

where *diff* is the unsigned difference between the orientations of the mask and target (in degrees) and h is the half-width at half-height of the excitatory tuning function (in degrees). We also assume that there is a detecting mechanism whose preferred orientation is matched to the target stimulus. Thus, the excitatory response (E) is given by

$$E = (C_t + MG)^p, \tag{4}$$

where C_t and M are the contrasts (in percent) of target and mask components, respectively, and p is an expansive exponent.

We propose a suppression function (L') that is a decreasing linear function of the difference between mask and target orientations:

$$L' = 1 - (diff/2|H|) \tag{5}$$

and

$$\text{IF } L' \geq 0 \text{ THEN } L = L' \text{ ELSE } L = 0. \tag{6}$$

This defines H as the half-width at half-height of the suppression function. Our results did not provide strong constraints on H, but preliminary analysis showed that good fits were possible for our data and those of Phillips and Wilson (1984) using H = ±65°, and this is what we used for the main analysis.

The function I (in Equation 2) is given by

$$I = (\gamma(C_t + MG) + wML)^q, \tag{7}$$

where q is an expansive exponent, γ is the weight of self-suppression, and w is the weight of the nonexcitatory route to suppression. Following earlier work (Legge & Foley, 1980), we set p = 2.4 and q = 2.0. The fact that the inhibitory terms are summed before being raised to the

power q means that this arrangement is similar to Foley's model 2.

To fit the model to the orientation-masking functions, Equation 2 was solved numerically for C_t to determine predictions for which

$$k = resp(\text{mask} + \text{target}) - resp(\text{mask}), \quad (8)$$

where k is the model criterion for detection, consistent with a late source of additive noise.

In fitting the results, C_t was calculated twice for each orientation, once with the mask contrast (M) set to 40% (C_{mask}) and once with the mask contrast (M) set to 0% ($C_{\text{no mask}}$) to predict threshold elevation, given by $20\log_{10}(C_{\text{mask}}/C_{\text{no mask}})$. There were four free parameters (h, w, γ, and k) for which values were determined by the simplex algorithm. The algorithm was started from several different sets of initial conditions and the reported values are those for which the RMS error of the fit was lowest. In most cases, the different starting conditions produced very similar results.

Model results

We concentrated our model analysis on the transient condition because this is where XOM was greatest. The fits are shown by the solid curves in Figures 2 and 3 (we did not attempt to fit the results for the 9 c/deg condition in Figure 2 since there was so little masking), and the parameters are reported in Table 1. Note that for each observer the weight of cross-orientation suppression (w) decreases with spatial frequency, consistent with previous analysis (Meese & Holmes, 2007). Note also that in Figures 3a–3d we show the threshold elevations anticipated by the model for the broader range of mask orientations not considered by Phillips and Wilson (1984).

Figure 4 shows the orientation bandwidths (h) estimated for the observers from Phillips and Wilson's (1984) study (SL and WS). The original study (open symbols; their Figure 4) reported that bandwidth decreases with spatial frequency. In general, this trend was not found here (filled symbols), which tended to be narrower than previous estimates. These results are replotted in Figure 5 (triangles and diamonds), along with those for TSM and DJH (circles and squares). On average, orientation bandwidth is about ±20° (mean = ±20.36°) for a four-octave range of spatial frequencies (0.5 to 8 c/deg; open circles in Figure 5). We do note, however, that although the (interpolated) average across the four observers (two from each study) shows no effect of spatial frequency, there is a slight downward trend for each observer across the lowest two spatial frequencies (for only one of these observers is the decline greater than 3°), suggesting that a weak effect might exist.

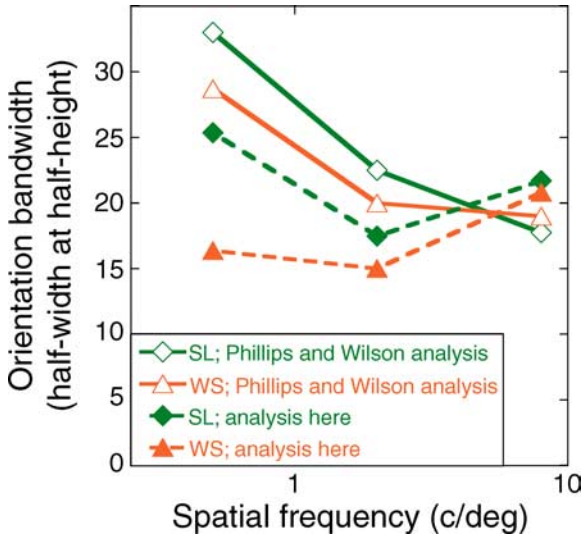

Figure 4. Estimates of orientation bandwidth (equivalent to h) for SL and WS from Phillips and Wilson (1984). See figure legend and text for details.

We also fitted our model with the cross-orientation suppression removed (i.e., $w = 0$) and for mask orientations restricted to the range 0–50° (similar to Phillips &

Obs	SF	RMS error (dB)	γ	w	k	$\pm h°$
DJH	1	0.70	6.21	0.63	0.02	18.22
DJH	3	0.78	1.31	0.26	0.82	15.98
TSM	1	0.63	2.24	0.48	0.24	29.13
TSM	3	0.49	0.69	0.18	1.76	26.32
SL	0.5	0.56	1.45	0.46	0.46	25.35
SL	2	1.07	1.00	0.09	1.40	17.48
SL	8	1.19	0.49	0.06	0.57	21.70
WS	0.5	0.56	2.72	0.37	0.12	16.37
WS	2	0.68	2.57	0.14	0.15	15.00
WS	8	1.20	0.53	0.06	0.52	20.80

Table 1. Quality of fit (RMS error) and parameter values of the functional model. Results are for the transient conditions from this study and Phillips and Wilson's (1984) study. The bandwidth (half-width at half-height) of broadly tuned suppression (H) was ±65°. The bandwidth (half-width at half-height) of excitation and self-suppression is given by h.

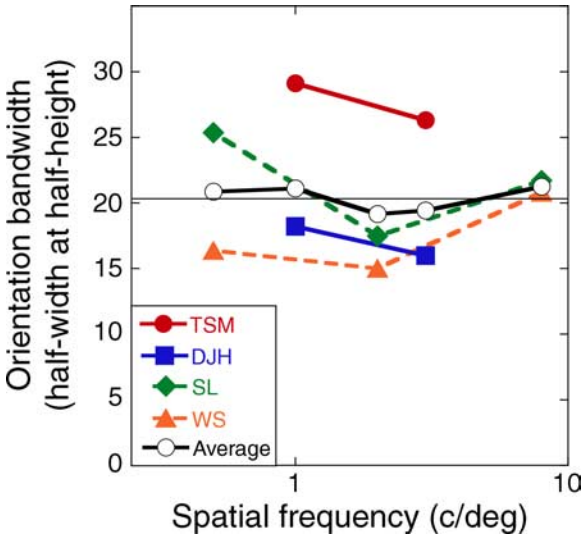

Figure 5. Estimates of orientation bandwidth (*h*) for four observers. TSM and DJH are from the present study. SL and WS are from Phillips and Wilson (1984) and are replotted from Figure 4. The open circles show the average of the four observers calculated using linear interpolation where appropriate. The thin horizontal line indicates the overall average.

Wilson's, 1984 range). This increased the estimate of orientation bandwidth markedly in all cases (by an average half-width of 9°) as shown in Figure 6. For the two observers from Phillips and Wilson's study (SL and WS), there is a downward trend of these differences with spatial frequency, consistent with the hypothesis that the spatial frequency dependency of filter bandwidth in Phillips and Wilson's study is, in fact, attributable to a spatial frequency dependency of XOS (Meese & Holmes, 2007). However, the opposite trend is seen for the two observers from the present study. We have no explanation for this difference across studies. However, we suggest that it is probably unwise to attach too much significance to the details of simple functional model fits when the model is clearly wrong (i.e., it contains no XOS). The main message from Figure 6 is that the exclusion of XOS is likely to lead to filter bandwidths being overestimated.

Further modeling involving multiple mechanisms and spatial summation

So far, the excitatory component of our model has involved only a single notional filter element that looks directly at the target. Of course, vision contains multiple filter elements in multiple filters and one question is whether pooling over space and filters will change our conclusions. We tackled this with more detailed modeling as follows.

We used an image-driven model with 18 oriented filters, area summation across filter elements within each filter, and Minkowski pooling across filters (see Appendix A for details). Although this general type of filter-based image-processing model is commonplace in contemporary work on spatial vision (e.g., Goris, Wichmann, & Henning, 2009; Meese, 2010; Párraga, Troscianko, & Tolhurst, 2005; Petrov, Dosher, & Lu, 2005; Rohaly, Ahumada, & Watson, 1997; To, Lovell, Troscianko, & Tolhurst, 2010; Watson & Ahumada, 2005; Watson & Solomon, 1997), we chose to avoid this for our initial analysis for the following reasons. First, we wanted to extend the Phillips and Wilson (1984) type of model in the simplest way possible (Equation 2) so as to examine the influence of XOS on previous estimates of orientation bandwidth. Second, the potentially large number of parameters and decisions about model construction (some of which are discussed below) mean that, arguably, this type of approach is overspecified for the main analysis here (only 2 model parameters were varied freely, but another 2 were adjusted by hand and a further 8 parameters were fixed, as we describe in Appendix A). Third, the time-consuming process of spatial filtering means that this approach is poorly suited to optimizing model parameters that are part of that filtering process (e.g., orientation bandwidth).

The filter model extends the functional model by performing spatial summation of each of the contrast terms on the numerator and denominator of the gain control equation across space and phase. Essentially, this extends the dilution masking and area summation model of Meese and Summers (2007) to include cross-orientation masking. Previous models of masking have usually either ignored area (spatial) summation (e.g., Itti, Koch, & Braun, 2000; Phillips & Wilson, 1984) or used the expedience of Minkowski summation over space (e.g., Watson &

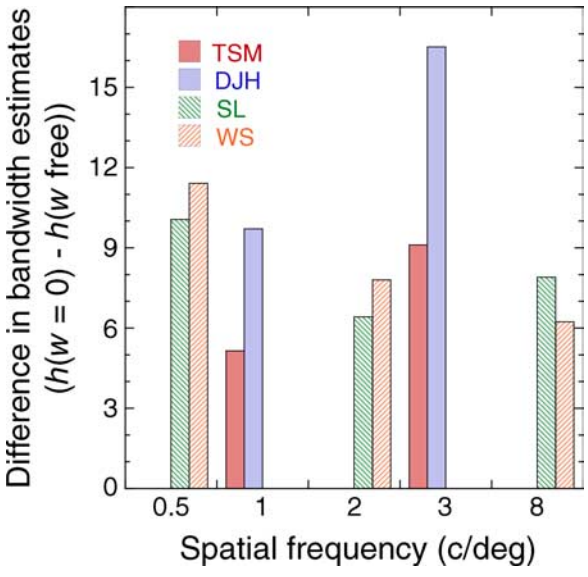

Figure 6. Signed differences between estimates in orientation bandwidth (*h*) with and without the inclusion of cross-orientation suppression. In all cases, the estimate of *h* was broader without cross-orientation suppression (i.e., the differences are all positive).

Solomon, 1997). Meese and Summers (2007) provided psychophysical evidence for a linear area summation process (following nonlinear transduction) that can extend up to at least 7 grating cycles at threshold and above (see also Meese, 2010; Meese & Baker, under review; Meese & Summers, 2009). This process is implemented as a spatial summation template in the model here (see Appendix A). The filter bandwidths of the 18 oriented filters were fixed at ±20° (at half-height) in accordance with our best overall estimate from the earlier analysis. The weight of each of these filter responses in each filter's divisive gain pool varied linearly with orientation difference and a bandwidth of H = ±65°, again consistent with the earlier analysis. There were four free parameters (the first three of which relate to the earlier model) as follows: (i) a sensitivity parameter k, (ii) the weight of the broadly tuned component of suppression (w), (iii) the weight of self-suppression γ, and (iv) a parameter, α, that controlled the spatial extent of the Gaussian summation template. The first two parameters were optimized; the second two were set by hand. Orientation pooling was performed using Minkowski summation of response differences to mask and mask-plus-target with an exponent of 2, broadly consistent with previous results (Meese, 2010).

The fits are shown for DJH and TSM in Figure 7 and are comparable with (sometimes better than) those achieved using the functional model (compare RMS errors in Tables 1 and 2). The solid red curves are for when the summation template was matched exactly to the envelope of the target (α = 1), the dashed blue curves are for when it was slightly larger (α = 1.5). The first point here is that our earlier analysis and claims are not undermined when the model is extended to include spatial summation and multiple spatial filters. For example, filter bandwidths of h = ±20° are consistent with all the results. Furthermore, because the model pools over 18 filter orientations, the analysis is not undermined by the strategy of off-channel looking (Blake & Holopigian, 1985).

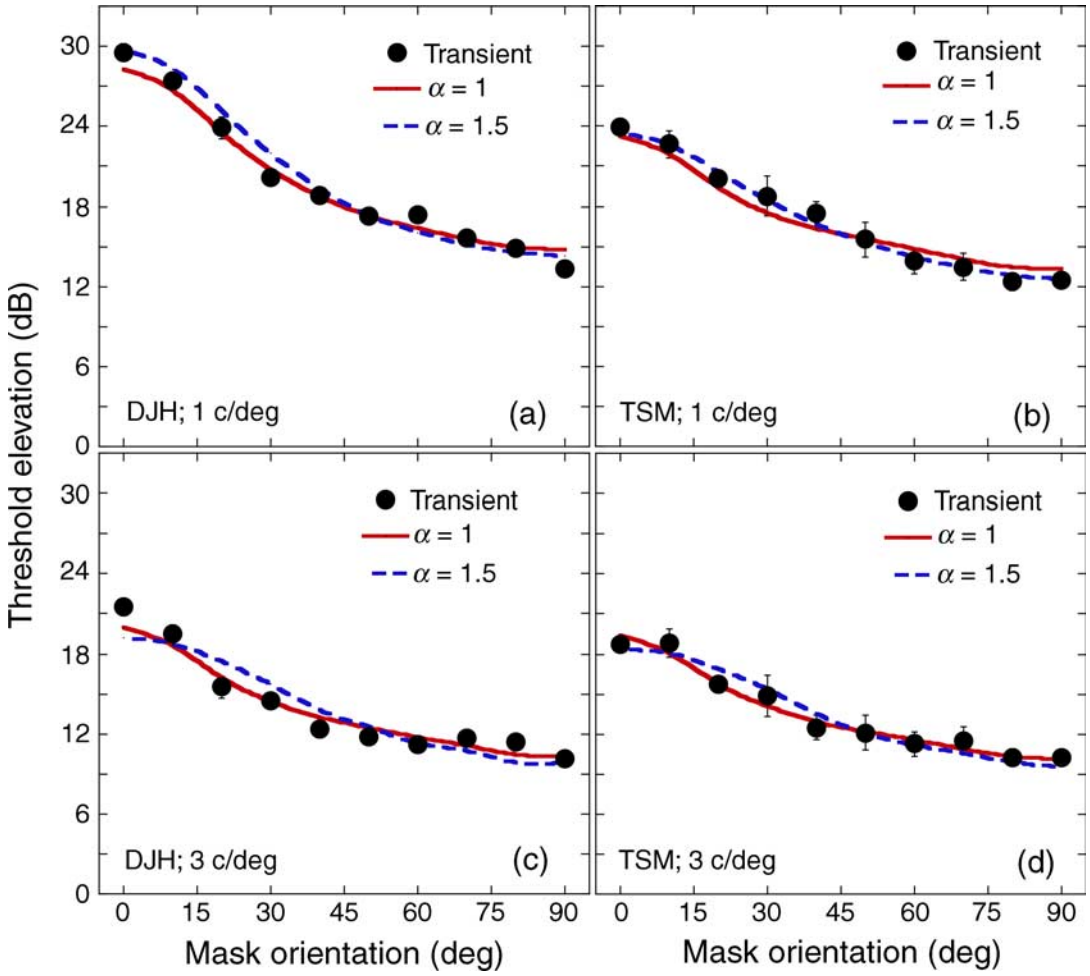

Figure 7. The transient contrast-masking results for DJH and TSM at 1 and 3 c/deg replotted from Figure 2. The curves are fits of the filter-based model with two parameters set by hand (γ and α) and two optimized (w and k). The size of the spatial template was set by the parameter α. For the solid red curve, it was matched to the size of the target region. For the blue dashed curve, it was larger. The orientation bandwidths of the filters were fixed at h = ±20° and the weight of broadly tuned suppression varied across relative orientation with a half-width (H) of ±65°.

Obs	SF	RMS error (dB)	γ	w	k	$\pm h°$
α = 1						
DJH	1	0.758	**100/*T***	$0.61/T^{1/q}$	$0.008T$	**20**
DJH	3	0.803	**10/*T***	$0.22/T^{1/q}$	$0.040T$	**20**
TSM	1	0.856	**10/*T***	$0.44/T^{1/q}$	$0.098T$	**20**
TSM	3	0.473	**10/*T***	$0.21/T^{1/q}$	$0.035T$	**20**
α = 1.5						
DJH	1	0.949	**100/*T***	$0.42/T^{1/q}$	$0.008T$	**20**
DJH	3	1.305	**10/*T***	$0.14/T^{1/q}$	$0.019T$	**20**
TSM	1	0.398	**10/*T***	$0.23/T^{1/q}$	$0.054T$	**20**
TSM	3	0.708	**10/*T***	$0.13/T^{1/q}$	$0.004T$	**20**

Table 2. Quality of fit (RMS error) and parameter values of the filter model for two different values of α. The bandwidth (half-width at half-height) of broadly tuned suppression (H) was ±65°. Other fixed parameters are shown in bold. T is a constant equal to the sum of the weights in a spatially matched template when $\alpha = 1$. It was included for numerical convenience and was unimportant for the fitting. The exponent $q = 2$.

Of particular note, the results for TSM are nicely described by this model, even with bandwidths that are markedly narrower than those estimated from the initial analysis (see Figure 5). At the lowest spatial frequency (1 c/deg), this was helped by using a spatial summation template that was larger than the target region ($\alpha > 1.0$). For the other thee data sets, the fits with $\alpha = 1.0$ were slightly better than those with $\alpha = 1.5$, though optimum fits probably lie in between (Table 2).

To demonstrate the effect of the spatial template parameter α more directly, we reran the model with fixed parameters, $h = \pm 20°$ and three different values of α (Figure 8). To test our functional model's susceptibility to variations in α (which was not part of that model), we then fitted our earlier model to the filter model curves in Figure 8 with the four free parameters as before (RMS error was always <0.36 dB; fits not shown). The bandwidths estimated from this fitting are termed h' and shown above each curve in Figure 8. The message is clear: compared to the filter model, the functional model tends to slightly overestimate bandwidth, and this error is worse when the spatial template exceeds the size of the target ($\alpha > 1$). Furthermore, forcing $h' = \pm 20°$ (the generating bandwidth for the curves in Figure 8) produced a good fit to the curve in Figure 8 for $\alpha = 1$, but the fits were unacceptable for the other two curves where $\alpha = 1.5$ and $\alpha = 2$ (fits not shown). Thus, if real observers use oversized spatial templates and their results are analyzed with a simple functional model, then it seems likely that their filter bandwidths will be overestimated.

General discussion

Summary of findings

We measured orientation-masking functions for two different forms of temporal modulation and a range of spatial frequencies (1–9 c/deg) for binocular grating masks and Gabor targets. We confirmed that XOM is greatest at low spatial frequencies and high temporal frequencies (Burbeck & Kelly, 1981; Medina & Mullen, 2009; Meese & Baker, 2009; Meese & Holmes, 2007).

We fitted a functional model of suppression to our main results and those of Phillips and Wilson (1984). From this, our estimates of filter bandwidths were less than previously estimated (Phillips & Wilson, 1984) at low spatial frequencies (about ±20°; see Figure 5) and showed little or no dependency on spatial frequency, depending on ones reading of Figure 5. A more realistic image-driven model

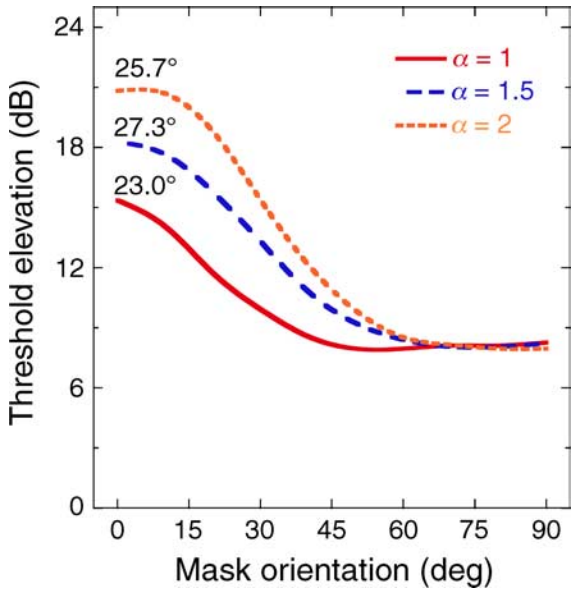

Figure 8. Behavior of the filter model (where $h = \pm 20$) for three different sizes of template (α). In this example, the cross-orientation suppression is strictly isotropic and the spatial template for this part of the model does not depend on α. The model curves were then fitted by the functional model with the orientation parameter (h') free. The estimated values of this parameter are shown above each curve.

was consistent with this conclusion and helped illustrate the influence of a mismatched spatial template.

Other masking studies and estimates of orientation bandwidth

Other studies closely related to ours are those of Phillips and Wilson (1984), Burbeck and Kelly (1981), Itti et al. (2000), Medina and Mullen (2009), Govenlock et al. (2009), Baker and Meese (2007), Foley (1994) and Cass et al. (2009). In the first two studies, the range of orientation differences was considerably less than ours (0°, 45° and 90°, respectively), and in the orientation-masking experiment performed by Itti et al., spatial and temporal frequencies were not manipulated. The study by Medina and Mullen measured coarsely sampled orientation-masking functions in the range 15°–90° but used only very low spatial frequencies (0.375–0.75 c/deg) and moderate temporal frequencies (2–4 Hz). The study by Govenlock et al. measured a wide range of mask orientations but, in most cases, did not measure sensitivity without a mask, so they could not assess XOM. Baker and Meese measured finely sampled orientation-masking functions but only for dichoptic stimuli and a target spatial frequency of 1 c/deg.

Cass et al. (2009) measured orientation-masking functions for monoptic and dichoptic masks and targets and also concluded that orientation bandwidth is invariant with spatial frequency. Their average estimate was broader than ours (h = ±30°), though it was based on descriptions of the threshold elevation functions rather than fitting a model. As mentioned in the Introduction section, it is to be expected that this will lead to broader estimates owing to the compressive nature of the psychophysical contrast response (Daugman, 1984; Phillips & Wilson, 1984). Our own estimates (±20°) are consistent with a recent estimate (±19°) that used a reverse-correlation technique (Roeber, Wong, & Freeman, 2008) and a spatial frequency of 2 c/deg. Essock, Haun, and Kim (2009) also measured masking functions using filtered noise masks and reported filter bandwidths of about ±20° at 8 c/deg. Campbell and Kulikowski (1966), Daugman (1984), and Harvey and Doan (1990) all used sine-wave gratings as masks and targets. Respectively, they found orientation bandwidths of ±13.6° at 8 c/deg, about ±12° to ±36° (depending on orientation) at 8 c/deg, and ±12° at 10 c/deg. It is unclear why the estimates from this last group of studies are so much narrower than the others. Overall then, there remains some uncertainty over the issue of orientation bandwidth at the higher spatial frequencies (8 c/deg and above).

Our models involve at least two components of suppression

The tightly tuned component of masking is well known (Campbell & Kulikowski, 1966), though not an explicit component in all models (Foley, 1994; Watson & Solomon, 1997). Increasingly, it is coming to be appreciated that this sits on a more broadly tuned component (Foley, 1994). Baker and Meese (2007) found similar results to those here for dichoptic masking (interocular suppression) and suggested that the threshold elevation functions might involve the combined influence of a tuned process and an isotropic process. Baker and Graff (2009) found a similar result for binocular rivalry. Cass et al. (2009) also described a tuned and an isotropic component of masking for both monoptic and dichoptic masking and Medina and Mullen (2009) found a similar result for binocular gratings. Medina and Mullen also measured orientation-masking functions for isoluminant (red/green) binocular gratings and found a purely isotropic effect. Roeber et al. (2008) used a reverse correlation technique to measure orientation interactions and concluded that there is an isotropic process of suppression for monoptic and dichoptic presentations. Ringach, Hawken, and Shapley (2003) used a reverse correlation technique with single-cell recordings. Similar to us, they concluded that there are two components of suppression: one tightly tuned, the other untuned. However, unlike in our models, their tuned component of suppression was slightly more broadly tuned than their excitatory component.

Here we have not attempted to determine the precise shape of the broadly tuned (untuned) effect. Visual inspection of the results at 1 c/deg (Figures 2a and 2b) provides a clear indication that the right-hand limb of the function is not flat but declines gently. This is why we chose a broad orientation-tuned component for our functional model (H = ±65°), which always produced (slightly) better fits than a flat isotropic process in that model (not shown). Similarly, Foley's (1994) broadly tuned suppression function declines gently with orientation difference between target and mask, though his function actually peaks at a 10° difference between the two. Watson and Solomon's (1997) suppression function is also a broadly tuned Gaussian, rather than a purely isotropic function. Nevertheless, these nuances represent minor detail variations across studies; it seems likely that our broad effect is of a similar origin to that of the effects described as isotropic in other studies.

Unlike us, Watson and Solomon (1997) did not include a tightly tuned component of suppression in their model. This possibly derives from the masking functions measured in Foley's (1994) and Foley and Boynton's (1994) studies, upon which the Watson and Solomon analysis was based. These are unusual when thresholds for high contrast masks are plotted as orientation-masking functions, since they show no evidence for a tightly tuned effect (see Figure 9).

It remains unclear why the form of the orientation-masking functions measured by Foley (1994) should be so different from most of those measured by Phillips and Wilson (1984) and many others, including us, but methodological differences might be important. For example, Foley varied the mask contrast (to measure

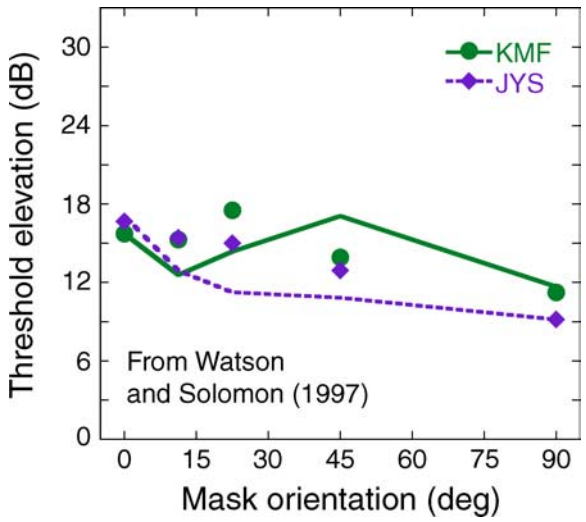

Figure 9. Orientation-masking functions for two observers from Foley and Boynton (1994) for a mask contrast of 31.6%. The mask was a sine-wave grating and the target was the Gabor patch in Figure 1. The spatial frequency was 2 c/deg and the stimulus duration was 33 ms. The data and model fits are replotted from Watson and Solomon (1997). The model contains no component of self-suppression other than that carried by the broadly tuned gain pool. Both model and data are extracted from a much larger data set where contrast-masking functions were measured for five different mask orientations. Thus, the model fits were constrained by many more data than those shown in this figure.

contrast-masking functions) whereas most other studies have kept this constant. However, how this might explain the different results is not clear either.

One, two, three, four, or five processes for orientation masking?

In principle, the tuned and isotropic components to masking (discussed above) might be a single process, arising from a common source such as inhibitory interactions between orientation-tuned cortical cells (DeValois, Yund, & Helper, 1982; Essock et al., 2009; Hansen & Essock, 2006; Haun & Essock, 2010; Heeger, 1992; Kim, Haun, & Essock, 2010; Ringach, Bredfeldt, Shapley, & Hawken, 2002). However, single-cell physiology provides evidence for an early isotropic process for contrast suppression (Bonin et al., 2005; Freeman, Durand, Kiper, & Carandini, 2002; Hirsch et al., 2003; Priebe & Ferster, 2006, 2008; Webb et al., 2005). If this were involved in the masking here, then it seems likely that a further process is responsible for the tightly tuned effect.

At this juncture then, we suppose two processes of suppression. The shapes of these functions and their sum are shown in Figure 10, where parameter values are fairly typical of those from our functional model. By implication, the tightly tuned component (long dashed (blue) curve) provides a direct indication of the orientation tuning of the detecting mechanism (filter). Indeed, this has been central (though sometimes implicit) to the motivation behind previous within-channel masking studies (e.g., Anderson & Burr, 1989; Daugman, 1984; Harvey & Doan, 1990; Phillips & Wilson, 1984) and it is an explicit component in our models. This is to say that the tightly tuned component of suppression owes purely to self-suppression from the target mechanism (or, equivalently, multiplicative noise). However, we know of no evidence to support this assumption and some single-cell evidence against it (Ringach et al., 2003). One possibility is that the tightly tuned component of suppression here might also involve inhibitory interactions *between* orientation-tuned mechanisms (Blakemore, Carpenter, & Georgeson, 1970; Carpenter & Blakemore, 1973; Heeger, 1992), which represents a third possible route to masking. We did not include it in our models here because (i) good fits to the data were achieved without it and (ii) it would introduce further free parameters. However, further modeling (not shown) confirmed that when such interactions were included, our estimates of orientation bandwidths (h) changed, typically increasing a little.

As in several other masking studies (Foley, 1994; Govenlock et al., 2009; Phillips & Wilson, 1984), our mask stimuli were larger than the target. Therefore, a

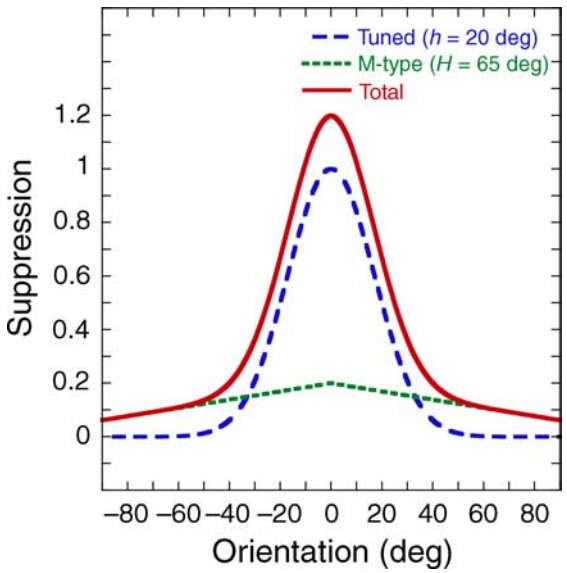

Figure 10. Orientation tuning of suppression in the model. The broadly tuned component (fine dashed green curve) has a weight of w = 0.2 and the tightly tuned component (coarse dashed blue curve) has a weight of γ = 1. This ratio of 1:5 is typical of that found in the functional model (Table 1). The sum of the two components of suppression (solid red curve) is also shown. For the functional model here, the excitatory passband of the filters had the same tuning as the tightly tuned component of suppression (coarse dashed blue curve). For the image-based model, the bandwidth was the same, but the shape differed in detail (it was a polar cross-section through a Cartesian separable log Gabor (see Appendix A and Meese, 2010).

fourth relevant route to masking here is surround suppression. Psychophysical evidence shows this to be orientation tuned and to saturate with contrast, but to be absent in the fovea at detection threshold (Meese, Challinor, Summers, & Baker, 2009; Petrov, Carandini, & McKee, 2005; Snowden & Hammett, 1998). However, surround contrast *can* suppress the detection of foveal contrast increments above threshold (Foley & Chen, 1999; Foley, 1994; Meese, 2004; Meese, Hess, & Williams, 2005). Thus, whatever the details of this interaction (e.g., see Meese et al., 2005), it is a potential pathway to suppression for the experiments here.

One further potential complication is that of *dilution masking* (Meese & Summers, 2007). This is a theoretical process that arises when excitation on the numerator of the contrast gain control equation extends to stimulus regions (in real space or Fourier space) that contain mask contrast but little or no target contrast and can result in masking (see Meese & Summers, 2007). As the relevant and irrelevant numerator terms each pass through their own accelerating contrast nonlinearity before summation, dilution masking is formally distinct from conventional within-channel masking (Meese & Summers, 2007). It is also distinct from cross-channel and pre-channel masking (see Introduction section) and surround suppression. The conditions needed for dilution masking could arise if stimulus summation extended into the surrounding mask region. In fact, this was an explicit feature of our filter-based model, determined by the parameter α (Appendix A). Whether this has been mistaken for pure surround suppression in other studies is not clear. However, in any case, our analysis (Figure 8) shows a relation between the effect of dilution masking and mask orientation (i.e., if dilution masking were involved in our (and other) experiments, then it would influence the shape of orientation-masking functions).

A general comment on orientation masking

The shape of the orientation-masking function depends on the interaction between excitation—which depends on the unknown filter bandwidth—and the orientation suppression function—whose shape is also unknown and could depend on several factors discussed above (self-suppression, tuned cortical interactions, the broadly tuned suppression field, surround suppression, and/or dilution masking). The experiments measure only the consequence of the interaction between excitation and total suppression, but neither in isolation. Only if the tuned component of the suppression function depends solely on self-suppression can data of this form constrain estimates of filter bandwidth.

What can orientation-masking studies tell us?

With possibly five different processes involved in suppression—potentially each having its own orientation tuning (see above)—we offer our estimate of the excitatory bandwidth parameter (h) with some caution. Performing experiments with masks and targets each of a similar size to the underlying receptive fields might avoid the problems associated with surround contrast but (i) the potentially complicating factor from tightly tuned cortical interactions would remain, (ii) dilution masking might still take place in the Fourier domain, and (iii) reducing the size of the mask would increase its bandwidth, thereby blurring the precision of the probe. Furthermore, single-cell studies in cats and monkeys imply that human vision contains mechanisms with a range of orientation bandwidths (DeValois, Albrecht et al., 1982; Ringach, Shapley, & Hawken, 2002; Tolhurst & Thompson, 1981; Yu et al., 2010), in which case, what does it mean to derive a single estimate of orientation bandwidth in this type of study? Presumably, orientation-masking studies will tend to tap detecting mechanisms at the narrower end of the distribution, since these will more readily escape the within-channel (self-suppression) effects of masking. Nevertheless, it seems likely that the estimate will represent some aggregate measure of mechanisms toward that end of the distribution.

Notwithstanding the above, the results here are of value. First and second, we have shown that cross-orientation suppression and dilution masking can influence estimates of filter bandwidth (Figures 4, 6, and 8). Third, we have shown that the spatial frequency dependency of filter orientation bandwidth is probably either weak, or absent, depending on one's reading of Figure 5. Fourth, we have shown that a filter-based model (Appendix A) involving spatial summation and dilution masking provides good fits to our transient results using filter bandwidths of ±20°. Fifth, we have shown that masking involves at least two components of suppression. It seems likely that these derive from distinct underlying processes, but this is not proven.

Filter-based image-processing models abound in vision science and its applications but rarely do they include mechanisms with multiple bandwidths. The results here provide some guidance on how bandwidths should be set in those models and offer some justification for the widely used practice of using the same bandwidths at each spatial scale. From our results, something in the region of ±20° is probably justifiable. However, bearing in mind that masking studies are likely to tap the narrower end of this distribution, an argument could be made for using slightly more broadly tuned filters.

Summation and adaptation studies

As discussed above, there are several problems involved in deriving quantitative estimates of mechanism bandwidth from masking studies. However, are other psychophysical methods better suited to this endeavor?

Subthreshold summation has been used to try and estimate orientation bandwidths. Early attempts used spatially extensive stimuli but neglected the effects of

spatial pooling (Kulikowski, Abadi, & Kingsmith, 1973), which led to very narrow estimates of orientation bandwidth (<5°). Subsequent work (e.g., Bergen, Wilson, & Cowan, 1979; Graham, 1989; Phillips & Wilson, 1984) showed that estimates become much broader when this is included, consistent with those from masking studies (Phillips & Wilson, 1984). However, another problem is that most work on subthreshold summation has assumed a linear contrast transducer, whereas an accelerating transducer is more likely (Lu & Dosher, 2008; Meese & Summers, 2009), which has important implications for pooling in the analysis (Meese, 2010; Meese & Summers, 2009). Thus, the questionable status of transduction and spatial probability summation (Meese, 2010; Meese & Summers, 2007, 2009; Watson & Ahumada, 2005; Watson & Solomon, 1997) and the narrow tuning of the empirical effects (when assessed with lines or gratings at least) mean that estimates of filter bandwidth have not been served well by this method. In fact, we are aware of no study that has used this method to assess orientation bandwidth as a function of spatial frequency for stationary grating-type stimuli. Whether some of these problems can be alleviated by using pairs of spatially localized Gabor patches (Watson, 1982) is not yet clear.

The method of contrast adaptation has also been used to assess the orientation bandwidths of adaptable cortical mechanisms (e.g., Snowden, 1992). Like early masking studies, results from this type of study also suggested that bandwidths are broader at lower spatial frequencies. However, it is now apparent that isotropic magnocellular cells in the LGN are also prone to contrast adaptation (Solomon et al., 2006; see also Camp, Tailby, & Solomon, 2009). Therefore, pre-channel cross-orientation adaptation aftereffects might be expected to increase estimates of bandwidth where the magnocellular stream dominates (high temporal and low spatial frequencies). Kelly and Burbeck (1987) performed psychophysical masking experiments and found results consistent with this hypothesis. Furthermore, Crowder et al. (2006) found that orientation-tuned cortical cells could be desensitized by adapting to orthogonal gratings for which they did not respond, just as we might expect if the isotropic pre-channel stage adapts. More generally though, a recent modeling study by Hegdé (2009) has shown that attempts to relate the tuning of adaptation aftereffects at the system level (psychophysics) and the single-cell level is fraught with difficulty and that, in general, the problem is ill-posed.

Loci of masking

The strong orientation tuning of masking points to a cortical origin for the suppression process associated with the parameter *h,* though whether this is placed at, before, or after the stage of binocular summation is not clear (Baker & Meese, 2007; Challinor, Meese, & Holmes, 2008; Moradi & Heeger, 2009).

The locus of the broadly tuned process associated with the parameter *H* is even less clear. It remains possible that it involves intra-cortical inhibition from oriented (Heeger, 1992; Ringach, Bredfeldt et al., 2002) or nonoriented mechanisms (Hirsch et al., 2003), but some recent single-cell physiology favors a subcortical isotropic locus (Bonin et al., 2005; Freeman et al., 2002; Priebe & Ferster, 2006, 2008; Webb et al., 2005; see also Meier & Carandini, 2002; though also Ringach & Malone, 2007). One possible way forward is to consider the psychophysical effects of interactions between the eyes, which are usually attributed to cortical processes. Although similarities have been found between monoptic and dichoptic XOM (Cass et al., 2009; Meese et al., 2008), these two forms of masking are clearly not the same in general (Meese & Baker, 2009; Baker, Meese, & Summers, 2007; Gheiratmand, Meese, & Mullen, 2009; Meese & Hess, 2004, 2005; Nichols & Wilson, 2009; Roeber et al., 2008), at least in the fovea. They have different spatiotemporal dependencies (Meese & Baker, 2009), different spatial frequency bandwidths, different time courses, and different susceptibilities to adaptation (Baker, Meese, & Summers, 2007). Although dichoptic XOM is typically stronger than the monoptic variety (Baker & Meese, 2007; Meese & Hess, 2004), there are clear examples where this is the other way around (Baker, Meese, & Summers, 2007; Meese & Baker, 2009). These numerous differences make a common post-binocular site for monoptic and dichoptic XOM extremely unlikely, at least as the sole cause of the broadly tuned effects. Thus, although cortical processes might be involved (this seems probable for dichoptic masking), it seems likely that the broadband/isotropic effect here asserts its influence before full binocular summation (Baker, Meese, & Summers, 2007). This suggests an early cortical stage at the latest (e.g., V1) but leaves open the possibility of a subcortical stage. On this view, the broadly tuned component might be attributed entirely to pre-channel masking (see Introduction section). We note that Klein, Carney, Barghout-Stein, and Tyler (1997) have made a similar point. If orientation filtering and an accelerating contrast response followed this stage, then this arrangement might also escape the arguments against the within-channel model reviewed in the Introduction section. In fact, recent developments in binocular contrast vision suggest multi-stage architectures (Baker, Meese, & Georgeson, 2007; Meese & Baker, under review; Meese et al., 2006) that might be developed as we propose.

Conclusions

Binocular threshold elevation for vertical targets by superimposed grating masks occurs for all mask orientations at low spatial frequencies and high temporal

frequencies. Psychophysical estimates of orientation bandwidths of transient mechanisms are narrower than once thought, around ±20° across a four-octave range of spatial frequencies (0.5 to 8 c/deg). Previous estimates of broader bandwidths owe to a failure to include cross-orientation suppression in the underlying model of masking. We suggest that at least two processes of suppression are involved. One is very potent and might have the same tuning as the excitatory passband of the detecting mechanism. The other is weaker, much more broadly tuned—almost isotropic—and is most prominent at low spatial frequencies and high temporal frequencies. Presumably, the first process is cortical, owing to the tight orientation tuning. The possibility remains that the second process is subcortical (producing pre-channel masking), at least for monocular pathways. However, a further three processes (tuned interactions, surround suppression, and dilution masking) can interfere with estimates of filter bandwidths in masking studies, including those reported here.

Appendix A

A filter-based model of masking and summation

This image-driven model extends the dilution masking and area summation model of Meese and Summers (2007) to include cross-orientation suppression and multiple spatial filters. We note that Petrov, Dosher et al. (2005) also performed linear spatial pooling over the target area within each filter but placed this operation *after* gain control and a sigmoidal output nonlinearity.

The gain control equation for the model filter responses used here was

$$resp_{\Theta} = \frac{\sum_{i=1:n} (|r_{S\Theta i}|^p + |r_{C\Theta i}|^p)}{1 + \gamma \sum_{i=1:n} (|r_{S\Theta i}|^q + |r_{C\Theta i}|^q) + \sum_{\tau=1:m} \left(\sum_{i=1:n} (|w\omega_\tau r_{S\tau i}|^q + |w\omega_\tau r_{C\tau i}|^q) \right)}, \quad \text{(A1)}$$

where the parameters were given as follows. The variable $resp_{\Theta}$ is the response of a single orientation-tuned filter with preferred orientation Θ following rectification and spatial pooling. Each of the n responses of the local filter elements at each point (i) in the image was weighted by a circular phase-insensitive spatial template with a two-dimensional Gaussian profile. The standard deviation of the template was $\alpha\sigma$, where σ is the standard deviation of the target stimulus in the experiment (σ = 0.708 cycles; Figure 1a) and α is a free parameter. When α = 1, the template was matched to the envelope of the signal. When $\alpha > 1$, the template was spatially more extensive than the signal. The template was insensitive to orientation, and the same spatial template was used to weight the responses from each of the 18 oriented filters.

After weighting by the template, the responses of the filter elements at location i are given by: $r_{S\theta i}$ and $r_{C\theta i}$ for the sine and cosine phase filters, respectively. (To avoid the tedium of using two-dimensional spatial subscripts, the weighting by the template is not explicit in our formal expressions.)

The exponents were set to p = 2.4 and q = 2, as in the functional model described in the main body of the report. The parameter γ controls the weight of self-suppression and was a free parameter. The rectified responses of the filter elements were raised to these powers before summation over area (i = 1 to n) and phase on both the numerator and denominator of the gain control equation (Equation A1). The suppressive gain pool also involved summation of the template-weighted sine and cosine phase filter elements at all n locations (i = 1 to n) and all m relative orientations (τ = 1 to m) each weighted further by ω_τ. These weights were set according to the gentle decline in sensitivity of the broadly tuned component of suppression given by the functional model in the main report (H = ±65°).

The spatial filters were Cartesian separable log Gabor filters with a spatial frequency bandwidth of 1.6 octaves and orientation bandwidth (at half-height) of ±20°. Meese (2010) provides the general equation for these filters. There were m = 18 pairs of filters (sine and cosine phases) spaced at intervals of 10° and centered on vertical (i.e., they sampled the full orientation domain in 10° steps). The response differences of these 18 filters across the 2AFC intervals were combined using Minkowski summation with an exponent of 2 to produce the decision variable. The model equations were solved for target contrast such that the target was detected when the decision variable exceeded a criterion level k that was related to the signal-to-noise ratio. This was performed with and without the mask to calculate threshold elevation.

Parameter summary

The four free parameters are: k, γ, w, and α (Table 2). The parameters γ and α were adjusted by hand to achieve acceptable fits. We did not experiment much with either parameter but found that the dilution masking produced by setting $\alpha > 1$ (see General discussion section) helped account for the different breadths of the tightly tuned effect across observers (TSM and DJH) while keeping the filter bandwidths constant. Therefore, we ran the model with α = 1.0 and α = 1.5. We were able to achieve good fits in most cases with $\gamma = 10/T$ but increased this to $\gamma = 100/T$ to fit the results for DJH at 1 c/deg, where the masking effects were particularly strong. The constant T

is the sum of the template weights for $\alpha = 1.0$, where there were 32 pixels per cycle of a sine-wave grating. The remaining parameters k and w were adjusted by an optimization routine (Matlab's *fmins*) to minimize the RMS error of the fit in dB.

The eight fixed parameters were: (i) the numerator exponent p, (ii) the denominator exponent q, (iii) the filter orientation bandwidth (h), (iv) the filter spatial frequency bandwidth (1.6 octaves), (v) the filter spacing (10°), (vi) the implicit relation between spatial pooling on the numerator and the denominator of the gain control equation (the spatial extent was the same), (vii) the relation between ω and τ (set according to $H = \pm 65°$), and (viii) the Minkowski summation exponent across filters (=2).

Acknowledgments

The data and functional modeling in this work were first reported in abstract form by Meese and Holmes (2003) and presented at the AVA Christmas Meeting at Aston University, UK (2002). The experimental work formed part of a doctoral thesis by the second author (Holmes, 2003).

The work was supported in part by two grants from the Engineering and Physical Sciences Research Council, UK (GR/S74515/01; EP/H000038/1) and a committee studentship awarded by the Biotechnology and Biological Sciences Research Council, UK.

We thank David Tolhurst and Josh Solomon for constructive criticism.

Commercial relationships: none.
Corresponding author: Dr. Tim S. Meese.
Email: t.s.meese@aston.ac.uk.
Address: Aston Triangle, Birmingham B4 7ET, UK.

References

Albrecht, D. G., & Geisler, W. S. (1991). Motion selectivity and the contrast response function of simple cells in the visual cortex. *Visual Neuroscience, 7,* 531–546.

Alitto, H. J., & Usrey, W. M. (2008). Origin and dynamics of extraclassical suppression in the lateral geniculate nucleus of the macaque monkey. *Neuron, 57,* 135–146.

Anderson, S. J., & Burr, D. C. (1989). Receptive field properties of human motion detection units. *Vision Research, 29,* 1343–1358.

Baker, D. H., & Graff, E. W. (2009). On the relation between dichoptic masking and binocular rivalry. *Vision Research, 49,* 451–459.

Baker, D. H., & Meese, T. S. (2007). Binocular contrast interactions: Dichoptic masking is not a single process. *Vision Research, 47,* 3096–3107.

Baker, D. H., Meese, T. S., & Georgeson, M. A. (2007). Binocular interaction: Contrast matching and contrast discrimination are predicted by the same model. *Spatial Vision, 20,* 397–413.

Baker, D. H., Meese, T. S., & Summers, R. J. (2007). Psychophysical evidence for two routes to suppression before binocular summation of signals in human vision. *Neuroscience, 146,* 435–448.

Baker, G. E., Thompson, I. D., Krug, K., Smyth, D., & Tolhurst, D. J. (1998). Spatial frequency tuning and geniculocortical projections in the visual cortex (areas 17 and 18) of the pigmented ferret. *European Journal of Neuroscience, 10,* 2657–2668.

Bergen, J. R., Wilson, H. R., & Cowan, J. D. (1979). Further evidence for four mechanisms mediating vision at threshold: Sensitivities to complex gratings and aperiodic stimuli. *Journal of the Optical Society of America A, 69,* 1580–1587.

Blake, R., & Holopigian, K. (1985). Orientation selectivity in cats and humans assessed by masking. *Vision Research, 25,* 1459–1467.

Blakemore, C., & Campbell, F. W. (1969). On existence of neurones in human visual systems selectively sensitive to orientation and size of retinal images. *The Journal of Physiology, 203,* 237–260.

Blakemore, C., Carpenter, R. H. S., & Georgeson, M. A. (1970). Lateral inhibition between orientation detectors in the human visual system. *Nature, 228,* 37–39.

Blakemore, C., & Nachmias, J. (1971). Orientation specificity of 2 visual after-effects. *The Journal of Physiology, 213,* 157.

Bonds, A. B. (1989). Role of inhibition in the specification of orientation selectivity of cells in the cat striate cortex. *Visual Neuroscience, 2,* 41–55.

Bonin, V., Mante, V., & Carandini, M. (2005). The suppressive field of neurons in lateral geniculate nucleus. *Journal of Neuroscience, 25,* 10844–10856.

Burbeck, C. A., & Kelly, D. H. (1981). Contrast gain measurements and the transient-sustained dichotomy. *Journal of the Optical Society of America, 71,* 1335–1342.

Burton, G. J. (1981). Contrast discrimination by the human visual system. *Biological Cybernetics, 40,* 27–38.

Camp, A. J., Tailby, C., & Solomon, S. G. (2009). Adaptable mechanisms that regulate the contrast response of neurons in the primate lateral geniculate nucleus. *Journal of Neuroscience, 29,* 5009–5021.

Campbell, F. W., & Kulikowski, J. J. (1966). Orientational selectivity of human visual system. *The Journal of Physiology, 187,* 437–445.

Carandini, M., Heeger, D. J., & Movshon, J. A. (1997). Linearity and normalization in simple cells of the macaque primary visual cortex. *Journal of Neuroscience, 17,* 8621–8644.

Carpenter, R. H. S., & Blakemore, C. (1973). Interactions between orientations in human vision. *Experimental Brain Research, 18,* 287–303.

Cass, J., Stuit, S., Bex, P., & Alais, D. (2009). Orientation bandwidths are invariant across spatiotemporal frequency after isotropic components are removed. *Journal of Vision, 9*(12):17, 1–14, http://www.journalofvision.org/content/9/12/17, doi:10.1167/9.12.17. [PubMed] [Article]

Challinor, K. L., Meese, T. S., & Holmes, D. J. (2008). A two-stage process for masking: Linear suppression is more broadly tuned than super-suppression. *Perception, 37,* 313. [Abstract] AVA Christmas Meeting.

Crowder, N. A., Price, N. S. C., Hietanen, M. A., Dreher, B., Clifford, C. W. G., & Ibbotson, M. R. (2006). Relationship between contrast adaptation and orientation tuning in V2 of cat visual cortex. *Journal of Neurophysiology, 95,* 271–283.

Daugman, J. G. (1984). Spatial visual channels in the Fourier plane. *Vision Research, 24,* 891–910.

DeValois, R. L., Albrecht, D. G., & Thorell, L. G. (1982). Spatial frequency selectivity of cells in macaque visual cortex. *Vision Research, 22,* 545–559.

DeValois, R. L., Yund, E. W., & Helper, N. (1982). The orientation and direction selectivity of cells in macaque visual cortex. *Vision Research, 22,* 531–544.

Essock, E. A., Haun, A. M., & Kim, Y. J. (2009). An anisotropy of orientation-tuned suppression that matches the anisotropy of typical natural scenes. *Journal of Vision, 9*(1):35, 1–15, http://www.journalofvision.org/content/9/1/35, doi:10.1167/9.1.35. [PubMed] [Article]

Ferrera, V. P., & Wilson, H. R. (1985). Spatial frequency tuning of transient non-oriented units. *Vision Research, 25,* 67–72.

Finney, D. J. (1971). *Probit analysis* (3rd ed.). London: Cambridge University Press.

Foley, J., & Chen, C. C. (1997). Analysis of the effect of pattern adaptation on pattern pedestal effects: A two-process model. *Vision Research, 37,* 2779–2788.

Foley, J., & Chen, C. C. (1999). Pattern detection in the presence of maskers that differ in spatial phase and temporal offset: Threshold measurements and a model. *Vision Research, 39,* 3855–3872.

Foley, J. M. (1994). Human luminance pattern-vision mechanisms: Masking experiments require a new model. *Journal of the Optical Society of America A, 11,* 1710–1719.

Foley, J. M., & Boynton, G. M. (1994). A new model of human luminance pattern vision mechanisms: Analysis of the effects of pattern orientation, spatial phase and temporal frequency. In T. B. Lawton (Ed.), *Computational vision based on neurobiology. Proceedings of SPIE 2054* (pp. 32–42).

Foley, J. M., & Legge, G. E. (1981). Contrast detection and near-threshold discrimination in human vision. *Vision Research, 21,* 1041–1053.

Freeman, T. C., Durand, S., Kiper, D. C., & Carandini, M. (2002). Suppression without inhibition in visual cortex. *Neuron, 35,* 759–771.

Georgeson, M. A., & Shackleton, T. M. (1994). Perceived contrast of gratings and plaids—Nonlinear summation across oriented filters. *Vision Research, 34,* 1061–1075.

Gheiratmand, M., Meese, T. S., & Mullen, K. T. (2009). Cross orientation masking in color vision: Cortical processing assessed with dichoptic presentation. Fall Vision Meeting Abstract [Abstract]. *Journal of Vision, 9*(14):84, 84a (Fall Vision Meeting, USA), doi: 10.1167/9.14.84, http://www.journalofvision.org/content/9/14/84.

Goris, R. L. T., Wichmann, F. A., & Henning, G. B. (2009). A neurophysiologically plausible population code model for human contrast discrimination. *Journal of Vision, 9*(7):15, 1–22, http://www.journalofvision.org/content/9/7/15, doi:10.1167/9.7.15. [PubMed] [Article]

Govenlock, S. W., Taylor, C. P., Sekuler, A. B., & Bennett, P. J. (2009). The effect of aging on the orientational selectivity of the human visual system. *Vision Research, 49,* 164–172.

Graham, N. (1989). *Visual pattern analyzers*. New York: Oxford University Press.

Greenlee, M. W., & Heitger, F. (1988). The functional-role of contrast adaptation. *Vision Research, 28,* 791–797.

Hansen, B. C., & Essock, E. A. (2006). Anisotropic local contrast normalization: The role of stimulus orientation and spatial frequency bandwidths in the oblique and horizontal effect perceptual anisotropies. *Vision Research, 46,* 4398–4415.

Harvey, L. O., & Doan, V. Y. (1990). Visual masking at different polar angles in the two-dimensional Fourier plane. *Journal of the Optical Society of America A, 7,* 116–126.

Haun, M., & Essock, A. (2010). Contrast sensitivity for oriented patterns in 1/*f* noise: Contrast response and

the horizontal effect. *Journal of Vision, 10*(10):1, 1–21, http://www.journalofvision.org/content/10/10/1, doi:10.1167/10.10.1. [Article]

Heeger, D. J. (1992). Normalization of cell responses in cat striate cortex. *Visual Neuroscience, 9,* 181–197.

Hegdé, J. (2009). How reliable is the pattern adaptation technique? A modeling study. *Journal of Neurophysiology, 102,* 2245–2252.

Hirsch, J. A., Martinez, L. M., Pillai, C., Alonso, J.-M., Wang, Q., & Sommer, F. T. (2003). Functionally distinct inhibitory neurons at the first stage of visual cortical processing. *Nature Neuroscience, 12,* 1300–1308.

Holmes, D. J. (2003). *Pooling and suppression in human vision*. PhD thesis, Aston University, UK.

Holmes, D. J., & Meese, T. S. (2004). Grating and plaid masks indicate linear summation in a contrast gain pool. *Journal of Vision, 4*(12):7, 1080–1089, http://www.journalofvision.org/content/4/12/7, doi:10.1167/4.12.7. [PubMed] [Article]

Houlihan, K., & Sekuler, R. (1968). Contour interactions in visual masking. *Journal of Experimental Psychology, 77,* 281–285.

Hubel, D. H., & Wiesel, T. N. (1959). Receptive fields of single neurones in the cats striate cortex. *The Journal of Physiology, 148,* 574–591.

Itti, L., Koch, C., & Braun, J. (2000). Revisiting spatial vision: Toward a unifying model. *Journal of the Optical Society of America A, 17,* 1899–1917.

Kelly, D. H., & Burbeck, C. A. (1987). Further evidence for a broad-band, isotropic mechanism sensitive to high-velocity stimuli. *Vision Research, 27,* 1527–1537.

Kim, Y. J., Haun, A. M., & Essock, E. A. (2010). The horizontal effect in suppression: Anisotropic overlay and surround suppression at high and low speeds. *Vision Research, 50,* 838–849.

Klein, S. A., Carney, T., Barghout-Stein, L., & Tyler, C. W. (1997). Seven models of masking. *SPIE Proceedings, Human Vision and Electronic Imaging II, 3016,* 13–24.

Kulikowski, J. J., Abadi, R., & Kingsmith, P. E. (1973). Orientational selectivity of grating and line detectors in human vision. *Vision Research, 13,* 1479–1486.

Legge, G., & Foley, J. (1980). Contrast masking in human vision. *Journal of the Optical Society of America A, 70,* 1458–1471.

Lu, Z. L., & Dosher, B. A. (2008). Characterizing observers using external noise and observer models: Assessing internal representations with external noise. *Psychological Review, 115,* 44–82.

Määttänen, L. M., & Koenderink, J. J. (1991). Contrast adaptation and contrast gain control. *Experimental Brain Research, 87,* 205–212.

Medina, J. M., & Mullen, K. T. (2009). Cross-orientation masking in human color vision. *Journal of Vision, 9*(3):20, 1–16, http://www.journalofvision.org/content/9/3/20, doi:10.1167/9.3.20. [PubMed] [Article]

Meese, T. S. (2004). Area summation and masking. *Journal of Vision, 4*(10):8, 930–943, http://www.journalofvision.org/content/4/10/8, doi:10.1167/4.10.8. [PubMed] [Article]

Meese, T. S. (2010). Spatially extensive summation of contrast energy is revealed by contrast detection of micropattern textures. *Journal of Vision, 10*(8):14, 1–21, http://www.journalofvision.org/content/10/8/14, doi:10.1167/10.8.14. [Article]

Meese, T. S., & Baker, D. H. (2009). Cross-orientation masking is speed invariant between ocular pathways but speed dependent within them. *Journal of Vision, 9*(5):2, 1–15, http://www.journalofvision.org/content/9/5/2, doi:10.1167/9.5.2. [PubMed] [Article]

Meese, T. S., & Baker, D. H. (under review). Cross-eyed and spaced-out: Cascading normalization achieves ocularity and area invariances in humans and a three-stage model of contrast gain control. *Journal of Vision*.

Meese, T. S., Challinor, K. L., & Summers, R. J. (2008). A common contrast pooling rule for suppression within and between the eyes. *Visual Neuroscience, 25,* 585–601.

Meese, T. S., Challinor, K. L., Summers, R. J., & Baker, D. H. (2009). Suppression pathways saturate with contrast for parallel surrounds but not for superimposed cross-oriented masks. *Vision Research, 49,* 2927–2935.

Meese, T. S., Georgeson, M. A., & Baker, D. H. (2006). Binocular contrast vision at and above threshold. *Journal of Vision, 6*(11):7, 1224–1243, http://www.journalofvision.org/content/6/11/7, doi:10.1167/6.11.7. [PubMed] [Article]

Meese, T. S., & Hess, R. F. (2004). Low spatial frequencies are suppressively masked across spatial scale, orientation, field position, and eye of origin. *Journal of Vision, 4*(10):2, 843–859, http://www.journalofvision.org/content/4/10/2, doi:10.1167/4.10.2. [PubMed] [Article]

Meese, T. S., & Hess, R. F. (2005). Interocular suppression is gated by interocular feature matching. *Vision Research, 45,* 9–15.

Meese, T. S., Hess, R. F., & Williams, C. B. (2005). Size matters, but not for everyone: Individual differences for contrast discrimination. *Journal of Vision, 5*(11):2,

928–947, http://www.journalofvision.org/content/5/11/2, doi:10.1167/5.11.2. [PubMed] [Article]

Meese, T. S., & Holmes, D. J. (2003). Orientation masking: Suppression and orientation bandwidth. *Perception, 32,* 388.

Meese, T. S., & Holmes, D. J. (2007). Spatial and temporal dependencies of cross-orientation suppression. *Proceedings of the Royal Society B, 274,* 127–136.

Meese, T. S., & Summers, R. J. (2007). Area summation in human vision at and above detection threshold. *Proceedings of the Royal Society B, 274,* 2891–2900.

Meese, T. S., & Summers, R. J. (2009). Neuronal convergence in early contrast vision: Binocular summation is followed by response nonlinearity and area summation. *Journal of Vision, 9*(4):7, 1–16, http://www.journalofvision.org/content/9/4/7, doi:10.1167/9.4.7. [PubMed] [Article]

Meese, T. S., Summers, R. J., Holmes, D. J., & Wallis, S. A. (2007). Contextual modulation involves suppression and facilitation from the center and the surround. *Journal of Vision, 7*(4):7, 1–21, http://www.journalofvision.org/content/7/4/7, doi:10.1167/7.4.7. [PubMed] [Article]

Meier, L., & Carandini, M. (2002). Masking by fast gratings. *Journal of Vision, 2*(4):2, 293–301, http://www.journalofvision.org/content/2/4/2, doi:10.1167/2.4.2. [PubMed] [Article]

Moradi, F., & Heeger, D. J. (2009). Inter-ocular contrast normalization in human visual cortex. *Journal of Vision, 9*(3):13, 1–22, http://www.journalofvision.org/content/9/3/13, doi:10.1167/9.3.13. [PubMed] [Article]

Morrone, M. C., Burr, D. C., & Maffei, L. (1982). Functional implications of cross-orientation inhibition of cortical visual cells: I. Neurophysiological evidence. *Proceedings of the Royal Society B, 216,* 335–354.

Movshon, J. A., & Blakemore, C. (1973). Orientation specificity and spatial selectivity in human vision. *Perception, 2,* 53–60.

Mullen, K. T., & Losada, M. A. (1994). Evidence for separate pathways for color and luminance detection mechanisms. *Journal of the Optical Society of America A, 11,* 3136–3151.

Nachmias, J., & Sansbury, R. V. (1974). Grating contrast: Discrimination may be better than detection. *Vision Research, 14,* 1039–1042.

Nichols, D. F., & Wilson, H. R. (2009). Effect of transient versus sustained activation on interocular suppression. *Vision Research, 49,* 102–114.

Nolt, M. J., Kumbhani, R. D., & Palmer, L. A. (2007). Suppression at high spatial frequencies in the lateral geniculate nucleus of the cat. *Journal of Neurophysiology, 98,* 1167–1180.

Pantle, A., & Sekuler, R. (1969). Contrast response of human visual mechanisms sensitive to orientation and direction of motion. *Vision Research, 9,* 397–406.

Párraga, C. A., Troscianko, T., & Tolhurst, D. J. (2005). The effects of amplitude-spectrum statistics on foveal and peripheral discrimination of changes in natural images, and a multi-resolution model. *Vision Research, 45,* 3145–3168.

Petrov, A. A., Dosher, B. A., & Lu, Z.-L. (2005). The dynamics of perceptual learning: An incremental reweighting model. *Psychological Review, 112,* 715–743.

Petrov, Y., Carandini, M., & McKee, S. (2005). Two distinct mechanisms of suppression in human vision. *The Journal of Neuroscience, 25,* 8704–8707.

Phillips, G. C., & Wilson, H. R. (1984). Orientation bandwidths of spatial mechanisms measured by masking. *Journal of the Optical Society of America A, 2,* 226–232.

Priebe, N. J., & Ferster, D. (2006). Mechanisms underlying cross-orientation suppression in cat visual cortex. *Nature Neuroscience, 9,* 552–561.

Priebe, N. J., & Ferster, D. (2008). Inhibition, spike threshold, and stimulus selectivity in primary visual cortex. *Neuron, 57,* 482–497.

Ramoa, A. S., Shadlen, M., Skottun, B. C., & Freeman, R. D. (1986). A comparison of inhibition in orientation and spatial-frequency selectivity of cat visual cortex. *Nature, 321,* 237–239.

Regan, D., & Regan, M. P. (1987). Spatial-frequency tuning and orientational tuning in pattern evoked potentials measured by nonlinear analysis—Orientation discrimination. *International Journal of Neuroscience, 34,* 235–236.

Ringach, D. L., Bredfeldt, C. E., Shapley, R. M., & Hawken, M. J. (2002). Suppression of neural responses to nonoptimal stimuli correlates with tuning selectivity in macaque V1. *Journal of Neurophysiology, 87,* 1018–1027.

Ringach, D. L., Hawken, M. J., & Shapley, R. M. (2003). Dynamics of orientation tuning in macaque V1: The role of global and tuned suppression. *Journal of Neurophysiology, 90,* 342–350.

Ringach, D. L., & Malone, B. J. (2007). The operating point of the cortex: Neurons as large deviation detectors. *Journal of Neuroscience, 27,* 7673–7683.

Ringach, D. L., Shapley, R. M., & Hawken, M. J. (2002). Orientation selectivity in macaque V1: Diversity and laminar dependence. *The Journal of Neuroscience, 22,* 5639–5651.

Roeber, U., Wong, E. M. Y., & Freeman, A. W. (2008). Cross-orientation interactions in human vision. *Journal of Vision, 8*(3):15, 1–11, http://www.journalofvision.

org/content/8/3/15, doi:10.1167/8.3.15. [PubMed] [Article]

Rohaly, A. M., Ahumada, A. J., Jr., & Watson, A. B. (1997). Object detection in natural backgrounds predicted by discrimination performance and models. 3225–3235.

Ross, J., & Speed, H. D. (1991). Contrast adaptation and contrast masking in human vision. *Proceedings of the Royal Society B, 246,* 61–69.

Ross, J., Speed, H. D., & Morgan, M. J. (1993). The effects of adaptation and masking on incremental thresholds for contrast. *Vision Research, 33,* 2051–2056.

Shapley, R. M., & Victor, J. D. (1978). The effect of contrast on the transfer properties of cat retinal ganglion cells. *Journal of Physiology, 285,* 275–298.

Snowden, R. J. (1992). Orientation bandwidth: The effect of spatial and temporal frequency. *Vision Research, 32,* 1965–1974.

Snowden, R. J., & Hammett, S. T. (1998). The effects of surround contrast on contrast thresholds, perceived contrast and contrast discrimination. *Vision Research, 38,* 1935–1945.

Solomon, S. G., Lee, B. B., & Sun, H. (2006). Suppressive surrounds and contrast gain in magnocellular-pathway retinal ganglion cells of macaque. *Journal of Neuroscience, 26,* 8715–8726.

Summers, R. J., & Meese, T. S. (2009). The influence of fixation points on contrast detection and discrimination of patches of grating: Masking and facilitation. *Vision Research, 49,* 1894–1900.

Thomas, J. P., & Gille, J. (1979). Bandwidths of orientation channels in human-vision. *Journal of the Optical Society of America, 69,* 652–660.

To, M. P. S., Lovell, P. G., Troscianko, T., & Tolhurst, D. J. (2010). Perception of suprathreshold naturalistic changes in colored natural images. *Journal of Vision, 10*(4):12, 1–22, http://www.journalofvision.org/content/10/4/12, doi:10.1167/10.4.12. [PubMed] [Article]

Tolhurst, D. J., & Heeger, D. J. (1997). Comparison of contrast normalization and threshold models of the responses of simple cells. *Visual Neuroscience, 14,* 293–309.

Tolhurst, D. J., & Thompson, I. D. (1981). On the variety of spatial-frequency selectivities shown by neurons in area-17 of the cat. *Proceedings of the Royal Society B: Biological Sciences, 213,* 183–199.

Tolhurst, D. J., Movshon, J. A., & Dean, A. F. (1983). The statistical reliability of signals in single neurons in cat and monkey visual cortex. *Vision Research, 23,* 775–785.

Watson, A. B. (1982). Summation of grating patches indicates many types of detector at one retinal location. *Vision Research, 22,* 17–25.

Watson, A. B., & Ahumada, A. J., Jr. (2005). A standard model for foveal detection of spatial contrast. *Journal of Vision, 5*(9):6, 717–740, http://www.journalofvision.org/content/5/9/6, doi:10.1167/5.9.6. [PubMed] [Article]

Watson, A. B., & Solomon, J. A. (1997). A model of visual contrast gain control and pattern masking. *Journal of the Optical Society of America A, 14,* 2379–2391.

Webb, B. S., Dhruv, N. T., Solomon, S. G., Tailby, C., & Lennie, P. (2005). Early and late mechanisms of surround suppression in striate cortex of macaque. *Journal of Neuroscience, 25,* 11666–11675.

Wilson, H. R. (1980). A transducer function for threshold and suprathreshold human vision. *Biological Cybernetics, 38,* 171–178.

Yu, H. H., Verma, R., Yang, Y., Tibballs, H. A., Lui, L. L., Reser, D. H., et al. (2010). Spatial and temporal frequency tuning in striate cortex: Functional uniformity and specializations related to receptive field eccentricity. *European Journal of Neuroscience, 31,* 1043–1062.

Zenger, B., & Sagi, D. (1996). Isolating excitatory and inhibitory nonlinear spatial interactions involved in contrast detection. *Vision Research, 36,* 2497–2513.